

Numerical investigation of the nonlinear heat diffusion equation with high nonlinearity on the boundary

M.A. Christou^a, C. Sophocleous^{a,*}, C.I. Christov^b

^a *Department of Mathematics and Statistics, University of Cyprus, CY 1678 Nicosia, Cyprus*

^b *Department of Mathematics, University of Louisiana at Lafayette, USA*

Abstract

A nonlinear heat diffusion problem is considered when the thermal conductivity and heat capacity are nonlinear functions of the temperature. At one of the boundaries a highly nonlinear condition is imposed involving both the flux and the temperature. We apply equivalence transformation which allows to reformulate the problem as an equation with linear diffusion for the transformed function. This gives a unique opportunity to create a specialized implicit finite difference scheme with internal iterations that faithfully represents the energy balance for the system. The equivalence transformation allows one to treat problems with plane, cylindrical, and spherical symmetry in an unified fashion. As a featuring example we consider two versions of the nonlinear boundary condition: energy absorption and energy input. We show that the latter leads to blow up of the solution at the boundary and identify the profile of the blowing-up solution.

© 2008 Elsevier Inc. All rights reserved.

Keywords: Nonlinear heat equations; Equivalence transformations; Numerical solutions

1. Introduction

In the last couple of decades, a considerable interest is developed in studying nonlinear diffusion equations. Such equations allow one to create more realistic models for heat conduction involving information about the dependence of the coefficients on the temperature. For example, the nonlinear diffusion equation

$$C(T) \frac{\partial T}{\partial t} = \frac{\partial}{\partial x} \left(K(T) \frac{\partial T}{\partial x} \right) \quad (1)$$

describes the heat conduction in a material, where T is the temperature, $K(T)$ is the thermal conductivity and $C(T)$ is the heat capacity [1,2]. We note that if $C(T) = 1$, then Eq. (1) becomes the well-known nonlinear diffusion

* Corresponding author.

E-mail address: christod@ucy.ac.cy (C. Sophocleous).

$$\frac{\partial T}{\partial t} = \frac{\partial}{\partial x} \left(K(T) \frac{\partial T}{\partial x} \right), \quad (2)$$

which have a number of applications in Mathematical Physics [3]. More generally, the heat-conduction problem is described by the equation

$$\rho(r)C(T) \frac{\partial T}{\partial t} = \frac{1}{r^m} \frac{\partial}{\partial r} \left(K(T)r^m \frac{\partial T}{\partial r} \right), \quad (3)$$

which models the temperature in a rectangular ($m = 0$), cylindrical ($m = 1$), or spherical ($m = 2$) coordinates [4–6]. In this paper we consider the general equation, Eq. (3), along with the initial and boundary conditions [7]

$$\text{I.C.: } T(r, t) = \tilde{c}, \quad (4)$$

$$\text{B.C.: } T_r(0, t) = 0, \quad K(T(1, t))T_r(1, t) = \sigma T^\beta(1, t). \quad (5)$$

Here \tilde{c} is a given constant and σ and β give different models of heat exchanged at the boundary. For instance, if $\sigma < 0$ and $\beta = 4$ one has the Stephan–Boltzmann model of surface emissivity. Conversely, if $\sigma > 0$, one has an energy input through the boundary. The last case is much less investigated and actually, the power β may not be the same as in the Stephan–Boltzmann model. Yet it seems important to gather some insight theoretically for the case with energy input. Hence, we consider two main cases: $\sigma = -1, \beta = 4$ and $\sigma = +1, \beta = 4$. More details about the mathematical formulation of this problem can be found in [8]. In this latter work, scaling groups were used to derive numerical solution for certain forms of $K(T), C(T)$ and $\rho(r)$.

2. Equivalence transformations

We consider the nonlinear diffusion equation

$$f(x)F(u)u_t = (g(x)D(u)u_x)_x, \quad (6)$$

which encompasses the different cases represented in Eq. (3).

The purpose of the present work is to derive local mappings that connects Eq. (6) to an equation of the same class. That is, we find transformations of the class

$$x' = P(x, t, u), \quad t' = Q(x, t, u), \quad u' = R(x, t, u)$$

that maps

$$f'(x')F'(u')u'_t = (g'(x')D'(u')u'_x)_{x'} \quad (7)$$

into (6). Such mappings are known as *equivalence transformations* [9]. They are formed by the non-degenerate point transformations in the space (x, t, u, f, g, F, D) , which are projectable on the space of (x, t, u) , i.e. they have the form

$$\begin{aligned} (x', t', u') &= (T^t, T^x, T^u)(x, t, u), \\ (f', g', F', D') &= (T^f, T^g, T^F, T^D)(x, t, u, f, g, F, D) \end{aligned}$$

and transform any equation of the class of Eq. (6) for the function $u = u(x, t)$ with arbitrary elements (f, g, F, D) into an equation of the form of Eq. (7) for the function $u' = u'(x', t')$ with new arbitrary elements (f', g', F', D') .

Without dwelling in the tedious details, we present the equivalence transformations we obtained for the class equation (6), namely

$$x' = P(x), \quad t' = c_1 t + c_2, \quad u' = R(u), \quad f' = \frac{f}{P_x}, \quad g' = \mu_1 g P_x, \quad F' = \frac{\mu_2 F}{R_u}, \quad D' = \frac{\mu_2 D}{c_1 \mu_1 R_u}, \quad (8)$$

where $P(x)$ and $R(u)$ are arbitrary functions of their arguments, and P_x and R_u are, respectively, their derivatives. Detailed description of the direct method for deriving equivalence transformations can be found in [10]. For more applications of equivalence transformation one can refer to the recent publications [11,12].

Now being reminded that Eq. (3) is a special case of Eq. (6) and employing the equivalence transformations, Eq. (8), we deduce that the transformation

$$x = \int r^{-m} dr, \quad u = \int C(T) dT, \tag{9}$$

maps Eq. (3) into

$$f(x) \frac{\partial u}{\partial t} = \frac{\partial}{\partial x} \left[D(u) \frac{\partial u}{\partial x} \right], \tag{10}$$

where

$$f(x) = r^{2m} \rho(r), \quad D(u) = \frac{K(T)}{C(T)}.$$

Equivalently, the transformation

$$x = \int r^{-m} dr, \quad u = \int K(T) dT \tag{11}$$

maps Eq. (3) into

$$f(x)D(u) \frac{\partial u}{\partial t} = \frac{\partial^2 u}{\partial x^2}, \tag{12}$$

where

$$f(x) = r^{2m} \rho(r), \quad D(u) = \frac{C(T)}{K(T)}.$$

Also we point out that the equivalence transformations can be employed to connect Eqs. (1) and (2).

The equivalence transformations enable us to simplify Eq. (3). Furthermore, in order to solve it numerically, we need to specify the forms of $K(T)$, $C(T)$ and $\rho(r)$. The functions $K(T)$ and $C(T)$ are of the form of power laws and ρ is chosen such that the reduced equation has constant coefficients.

We note that Eq. (10) and/or Eq. (12) becomes the linear heat equation if $D(u) = f(x) = 1$. Hence, Eq. (3) can be linearized by local mappings if $K(T) = C(T)$ and $\rho(r) = r^{-2m}$.

Here we consider

$$K(T) = K_0 T^s, \quad C(T) = C_0 T^p,$$

which gives

$$D(u) = \frac{C_0}{K_0} T^{p-s}$$

and using transformation (11) we get

$$T = \sqrt[s+1]{\frac{s+1}{K_0} u} \quad \text{and} \quad D(u) = \frac{C_0}{K_0} \left(\frac{s+1}{K_0} u \right)^{\frac{p-s}{s+1}}. \tag{13}$$

Furthermore, we assume that $f(x) = 1$. Hence we obtain the following initial-boundary value problem:

$$((s+1)u)^{\frac{p-s}{s+1}} u_t = u_{xx} \tag{14}$$

with the following boundary and initial conditions:

- B.C.: if $m = 0$: $u_x = \sigma[(s+1)u]^{\frac{4}{s+1}}$ at $x = 1$ and $u_x = 0$ at $x = 0$,
- if $m = 1$: $u_x = \sigma[(s+1)u]^{\frac{4}{s+1}}$ at $x = 0$ and $u_x = 0$ when $x \rightarrow -\infty$,
- if $m = 2$: $u_x = \sigma[(s+1)u]^{\frac{4}{s+1}}$ at $x = -1$ and $u_x = 0$ when $x \rightarrow -\infty$,
- I.C.: $u(x, 0) = c = \text{constant}$.

It is convenient to rewrite Eq. (14) in the form

$$\frac{1}{p+1} \left\{ [(s+1)u]^{p+1} \right\}_t = u_{xx}, \quad (15)$$

which will allow us to create an adequate approximation of the time derivative.

We further set $v = (s+1)u$ and $\alpha = (p-s)/(s+1)$ to obtain the following initial-boundary value problem:

$$\frac{1}{(p+1)} (v^{p+1})_t = v_{xx} \quad (16)$$

with the boundary and initial conditions:

$$\begin{aligned} \text{if } m=0: & \quad v_x = -\sigma v^{\frac{4}{s+1}} \text{ at } x=1 \text{ and } v_x = 0 \text{ at } x=0, \\ \text{B.C.: if } m=1: & \quad v_x = -\sigma v^{\frac{4}{s+1}} \text{ at } x=0 \text{ and } v_x = 0 \text{ when } x \rightarrow -\infty, \end{aligned} \quad (17)$$

$$\begin{aligned} \text{if } m=2: & \quad v_x = -\sigma v^{\frac{4}{s+1}} \text{ at } x=-1 \text{ and } v_x = 0 \text{ when } x \rightarrow -\infty, \\ \text{I.C.: } & \quad v(x,0) = (s+1)c \quad (c = \text{constant}). \end{aligned} \quad (18)$$

In cylindrical and spherical coordinate systems the corresponding domains are $[-\infty, 0]$ and $[-\infty, -1]$, respectively. Then one can consider numerically finite intervals, such as $[-L_1, 0]$ and $[-L_2, -1]$ with $L_1, L_2 > 0$.

3. Energy balance

One of the most important results from the equivalence transformation is that the transformed initial-boundary value problem (i.b.v.p.) possesses a balance law for the energy. The following theorem holds:

Theorem 1. *The solution of the initial boundary value problem, Eqs. (14), (17) and (18), satisfying the following balance law is*

$$\frac{dh}{dt} \int_0^1 v^{z+2} dx = -\frac{(p+1)(\alpha+2)}{\alpha+1} \left[-\int_0^1 (v_x)^2 dx + \sigma v^{\frac{5+s}{1+s}} \right]. \quad (19)$$

Proof. We perform the differentiation in left-hand side of Eq. (16), multiply the latter by v and integrate with respect to x . For the left-hand side we get

$$\int_0^1 \frac{\alpha+1}{p+1} v \cdot v^z v_t dx = \int_0^1 \frac{\alpha+1}{(p+1)(\alpha+2)} \int_0^1 [v^{z+2}]_t dx = \frac{\alpha+1}{(p+1)(\alpha+2)} \frac{d}{dt} \int_0^1 v^{z+2} dx. \quad (20)$$

For the term in the right-hand side we get

$$\int_0^1 v v_{xx} dx = v v_x \Big|_0^1 - \int_0^1 (v_x)^2 dx = \sigma v^{\frac{5+s}{1+s}} - \int_0^1 (v_x)^2 dx, \quad (21)$$

which proves the statement of the theorem. \square

The initial boundary value problem, Eqs. (14), (17) and (18), is highly nonlinear for the time derivative and a solution can be obtained only numerically. To this end we use an implicit finite difference scheme in order to ensure both the stability and the satisfaction of the integral balances Eq. (16).

We introduce a fully implicit finite difference scheme which resembles the energy of the system. The nonlinear term in the evolution equation and on the boundary is being treated by internal iterations which are contacted until convergence. An implicit numerical scheme with internal iterations and satisfaction of balance law was used in [13] where the quenching (inverse process of nonlinear blow-up) was studied for a nonlinear diffusion equation. Moreover we show that our difference scheme represents the energy balance and prove that any leakage or gain of energy is not a defect of the numerical method but rather a physical consequence of the different terms of the model.

4. Difference scheme

We consider an uniform but spatially staggered grid

$$x_i = -\frac{h}{2} + ih \quad \text{for } i = 0, 1, \dots, N + 1, \quad h \equiv \frac{1}{N}, \tag{22}$$

which allows us to construct second-order approximations of the boundary conditions on two-point stencils.

To construct the numerical scheme we follow the spirit of the scheme from [13] modifying the details where necessary. We denote by τ the time increment. The superscript n on the time variable t stands for the current (old) time stage, and $n + 1$ for the new one. We use the following scheme which is a nonlinear modification of the Crank–Nicolson scheme:

$$\frac{1}{\tau(p + 1)} \frac{2}{v_i^{n+1,k} + v_i^n} [(v_i^{n+1,k})^{x+1} v_i^{n+1,k+1} - (v_i^{n+1,k})^{x+1} v_i^n] = \frac{1}{2} \mathcal{A}[v_i^{n+1,k+1} + v_i^n], \tag{23}$$

where \mathcal{A} is the difference operator defined for an arbitrary grid function ϕ_i as

$$\mathcal{A}\phi_i = \frac{\phi_{i+1} - 2\phi_i + \phi_{i-1}}{h^2}. \tag{24}$$

Note that in Eq. (23) we have introduced internal iterations. Similarly, for the nonlinear boundary condition at $x = 1$, we use the following implementation involving internal iterations:

$$v_{N+1}^{n+1,k+1} - v_N^{n+1,k+1} = -\frac{h}{2} \sigma \epsilon \left[(v^{n+1,k})^{\frac{3-\epsilon}{s+1}} v_N^{n+1,k+1} + v^{n+1,k} \right]^{\frac{3-\epsilon}{s+1}} v_{N+1}^{n+1,k+1}. \tag{25}$$

Finally, the boundary condition at $x = 0$ is simply approximated as

$$v_1^{n+1,k+1} - v_0^{n+1,k+1} = 0. \tag{26}$$

The approximation of the initial condition is obvious.

The internal iterations are repeated until convergence is reached in the sense that

$$\frac{\max_i \|v_i^{n+1,k+1} - v_i^{n+1,k}\|}{\max_i \|v_i^{n+1,k+1}\|} < \delta, \tag{27}$$

where δ is the specified accuracy of the iterations (say 10^{-10}). Thus at each iteration for the unknown function $v_i^{n+1,k+1}$ we solve a *linear* boundary value problem which reduces to a linear algebraic system with tri-diagonal matrix.

When the internal iterations converge, we get the solution of the full nonlinear implicit scheme

$$\frac{1}{\tau(p + 1)} \frac{2}{v_i^{n+1} + v_i^n} [(v_i^{n+1})^{x+2} - (v_i^n)^{x+2}] = \frac{1}{2} \mathcal{A}[v_i^{n+1} + v_i^n] \tag{28}$$

with the symmetry condition at $x = 0$

$$v_2^{N+1} = v_1^{N+1}, \tag{29}$$

and with a nonlinear b.c. at $x = 1$

$$v_{N+1}^{n+1} - v_N^{n+1} = \sigma \frac{h}{2} \left[(v^{n+1})^{\frac{4}{s+1}} \Big|_N + (v^{n+1})^{\frac{4}{s+1}} \Big|_{N+1} \right]. \tag{30}$$

5. Difference representation of the energy balance

We show that the discrete problem represents the energy balance of the continuous problem.

Theorem 2. For the difference scheme, Eq. (28), the following integral identity holds:

$$\begin{aligned}
& \frac{1}{\tau(s+1)(p+1)} \left[\sum_{i=2}^{N-1} h(v_i^{n+1})^{\alpha+2} - \sum_{i=2}^{N-1} h(v_i^n)^{\alpha+2} \right] \\
&= -\frac{1}{2} \sum_{i=2}^{N-1} \left[h \left(\frac{v_i^{n+1} - v_{i+1}^{n+1} + v_i^n - v_{i+1}^n}{2h} \right)^2 + h \left(\frac{v_i^{n+1} - v_{i-1}^{n+1} + v_i^n - v_{i-1}^n}{2h} \right)^2 \right] \\
& \quad + \frac{1}{2} \sigma(s+1)^{\frac{s+5}{s+1}} \left(\frac{v_N^{n+1} + v_{N-1}^{n+1} + v_N^n + v_{N-1}^n}{4} \right)^{\frac{s+5}{s+1}}. \tag{31}
\end{aligned}$$

Proof. Define the discrete scalar product as follows:

$$(\phi, \psi) = \sum_{i=2}^{N-1} h \phi_i \psi_i.$$

Then, following [13,14] we can show that

$$\begin{aligned}
(\phi, A\phi) &= \sum_{i=2}^{N-1} h v_i \left[\frac{\phi_{i+1} - 2\phi_i + \phi_{i-1}}{h} \right] = \sum_{i=2}^{N-1} h \left[\phi_i \left(\frac{\phi_{i+1} - \phi_i}{h} \right) + \phi_i \left(\frac{-\phi_i + \phi_{i-1}}{h} \right) \right] \\
&= -\frac{1}{2} \sum_{i=2}^{N-1} h \left[\frac{\phi_i^2 + v_{i+1}^2 - 2\phi_i \phi_{i+1}}{h^2} \right] - \frac{1}{2} \sum_{i=2}^{N-1} h \left[\frac{\phi_i^2 + v_{i-1}^2 - 2\phi_i \phi_{i-1}}{h^2} \right] + \frac{1}{2} \left(-\frac{\phi_{N-1}^2}{h} + \frac{\phi_N^2}{h} + \frac{\phi_1^2}{h} - \frac{\phi_2^2}{h^2} \right) \\
&= -\frac{1}{2} \sum_{i=2}^{N-1} h \left[\frac{\phi_{i+1} - \phi_i}{h} \right]^2 - \frac{1}{2} \sum_{i=2}^{N-1} h \left[\frac{\phi_i - \phi_{i-1}}{h} \right]^2 + \frac{1}{2} \frac{(\phi_N - \phi_{N-1})(\phi_N + \phi_{N-1})}{h} \\
& \quad - \frac{1}{2} \frac{(\phi_2 - \phi_1)(\phi_2 + \phi_1)}{h}.
\end{aligned}$$

From the boundary conditions, Eqs. (29) and (30), we get

$$\phi_1^2 = \phi_2^2, \quad \frac{1}{2} [\phi_N^2 - \phi_{N-1}^2] = \sigma h(s+1)^{\frac{4}{s+1}} \left(\frac{\phi_N + \phi_{N-1}}{2} \right)^{\frac{4}{s+1}} \frac{\phi_N + \phi_{N-1}}{2}. \tag{32}$$

Then for the above scalar product we get

$$(\phi, A\phi) = -\frac{1}{2} \sum_{i=2}^{N-1} \left[h \left(\frac{\phi_i - \phi_{i+1}}{h} \right)^2 + h \left(\frac{\phi_i - \phi_{i-1}}{h} \right)^2 \right] + \frac{1}{2} \sigma(s+1)^{\frac{4}{s+1}} \left(\frac{\phi_N + \phi_{N-1}}{2} \right)^{\frac{s+5}{s+1}}. \tag{33}$$

The term containing the time derivative is nonlinear which makes our scheme to faithfully represent the properties of the original initial-boundary value problem, e.g., the energy integral. To prove that we multiply both sides of Eq. (28) by h and take the sum from $i = 2$ to $i = M - 1$. Thus, we get

$$\frac{4}{\tau(s+1)(p+1)} \left[\sum_{i=2}^{N-1} h(v_i^{n+1})^{\alpha+2} - \sum_{i=2}^{N-1} h(v_i^n)^{\alpha+2} \right] = ([v_i^{n+1} + v_i^n], A[v_i^{n+1} + v_i^n]). \tag{34}$$

Introducing in the right-hand side of Eq. (33) written for the function $\phi = v^{n+1} + v^n$ we arrive at the statement of the Theorem.

Thus we have a scheme that emulates the respective property of the differential boundary value problem. In the other words, the energy-like sum (“functional”) evolves because of the (un)balance of the dissipation and energy production at the boundary with the nonlinear boundary condition. In this sense, our scheme does not contribute artificial (scheme) properties. \square

6. Numerical results

First, we elucidate the time evolution of the solution. As above mentioned, we consider two cases: emissive boundary condition (energy flows out of the boundary: $\sigma = -1$) and energy input: $\sigma = 1$. For the former

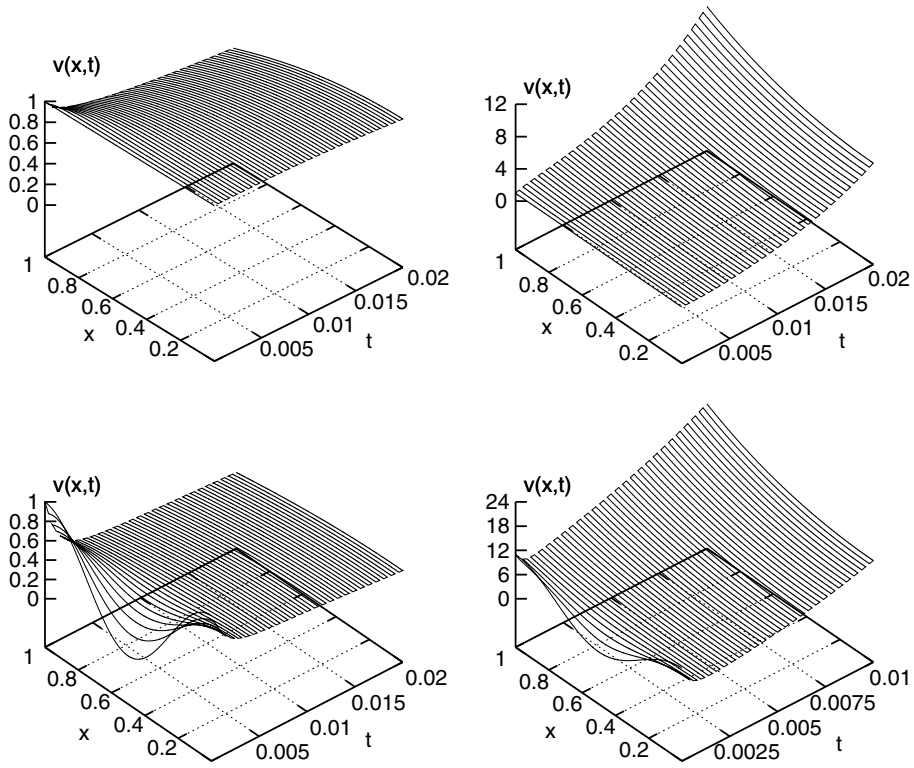


Fig. 1. Time evolution of $v(x,t)$. Left panels: surface emissivity with the $s = 4$ and $p = 10$. Right panels: energy input at the boundary for $s = 6$ and $p = 10$. Upper panels: constant initial condition. Lower panels: oscillating initial condition.

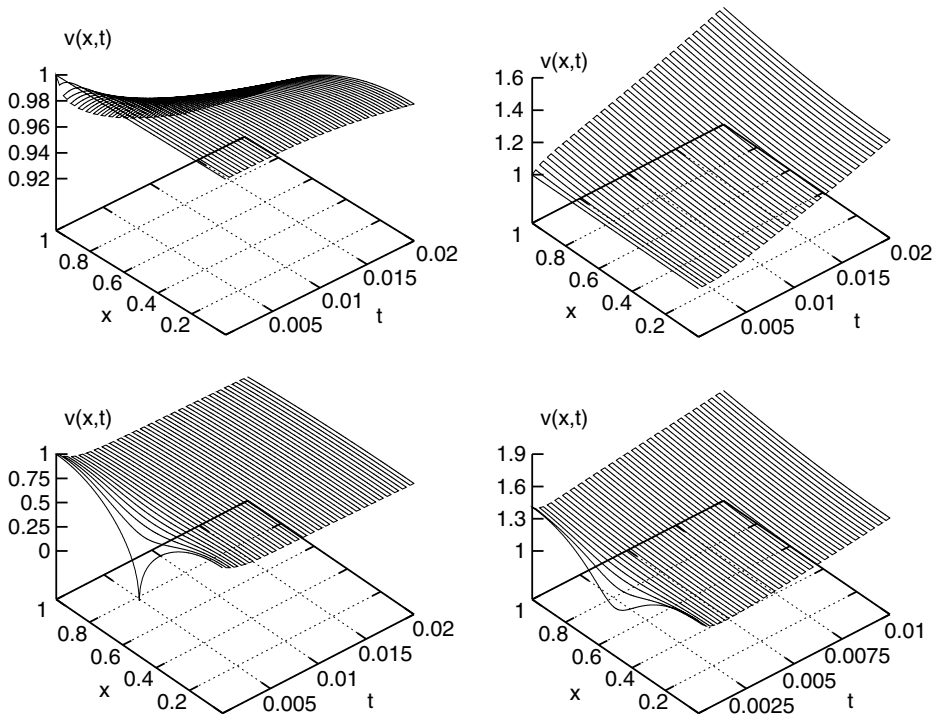


Fig. 2. Time evolution of $T(r,t)$. Left panels: surface emissivity with the $s = 4$ and $p = 10$. Right panels: energy input at the boundary for $s = 6$ and $p = 10$. Upper panels: constant initial condition. Lower panels: oscillating initial condition.

we chose the parameters to be $s = 4, p = 10$. For the latter we have $s = 6, p = 10$. We consider two different initial conditions. The first is the constant $v = 1$ and the second involves a non-monotone dependence on x .

In the upper left panel of Fig. 1 we show the case of constant initial condition $v(x, 0) = 1$ and emissivity b.c. In this case the function eventually decays to zero in time. The conspicuous trait here is that the decay is faster near the boundary with the emissivity condition. The lower left panel shows the same case but for non-monotone initial condition $v(x, 0) = \cos^2(\pi x)$. It is seen that the wavy initial condition is quickly flattened and after that the evolution continues as in the previous case and the solution slowly decays to zero.

The upper right panel of Fig. 1 shows the case with energy input for constant initial condition $v(x, 0) = 1$. In this case, the profile is blowing up exponentially. The speed of blow-up is faster near the b.c. with the energy input. We fitted curves to the obtained profile and found them to be exponential functions of time. It is seen that once again the faster evolution (in this case, the faster blow-up) takes place near the boundary with the nonlinear b.c. In the lower right panel of Fig. 1 we present the case when the initial condition is non-constant, namely $v(x, 0) = 1 + 10 \cos^2(\pi x)$. We take a larger initial condition to test the role of nonlinearity. Indeed, the blow-up is now much faster while the general tendency is preserved that the evolution near the boundary with nonlinear boundary condition is preserved. An important characteristics of the dynamics with non-monotone initial condition is that the diffusion process is much faster for the selected set of parameters, and for relatively small times the initial profile is flattened. Then at longer times the nonlinear boundary condition is felt and the dynamics is dominated by it.

Now, we derive the corresponding results for the original equation (3). We can transform the above numerical results for $T(r, t)$, using the inverse transformation of (11). Since $m = 0$ and $K(T) = T^s$, the inverse of (11) reads

$$r = x, \quad T(r, t) = \sqrt[s+1]{(s+1)u(x, t)} = \sqrt[s+1]{v(x, t)}.$$

The corresponding plots of $T(r, t)$ are demonstrated in Fig. 2.

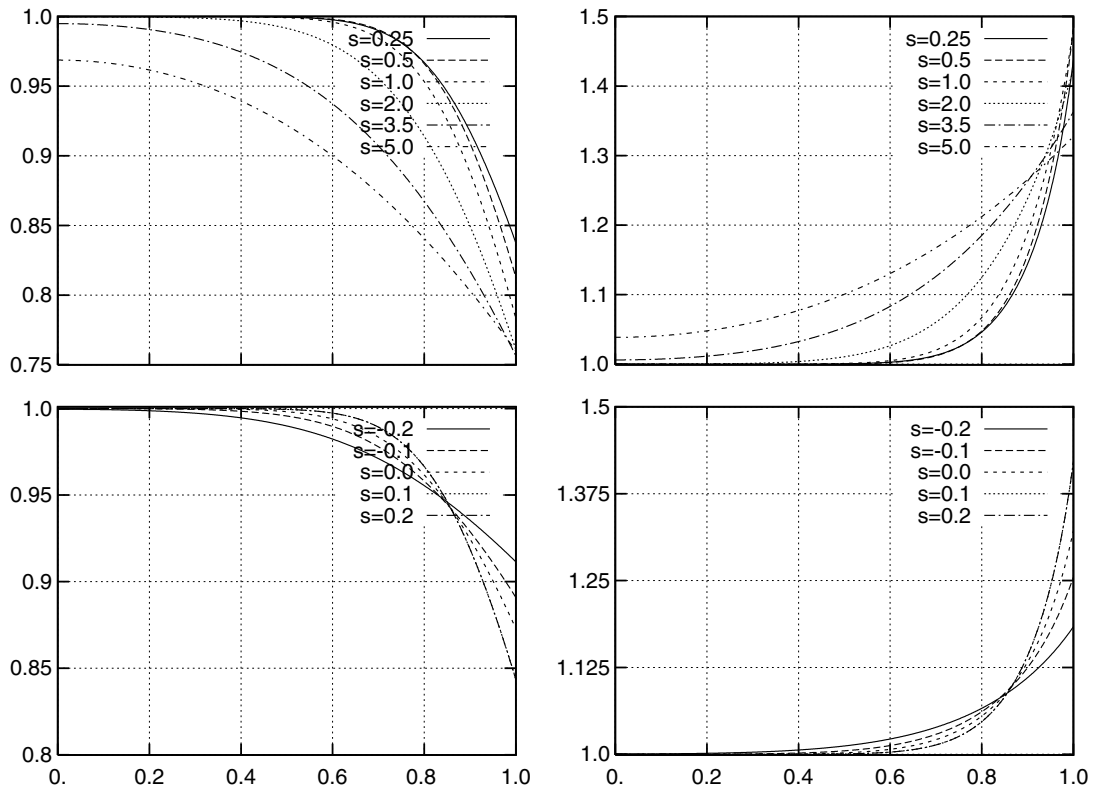


Fig. 3. The profiles of v for $p = 4$ and $t = 0.05$. Upper panels: $0.25 \leq s \leq 5$ Lower panels: $-0.2 \leq s \leq 0.2$. Left panels: emissivity b.c. Right panels: energy input at the boundary.

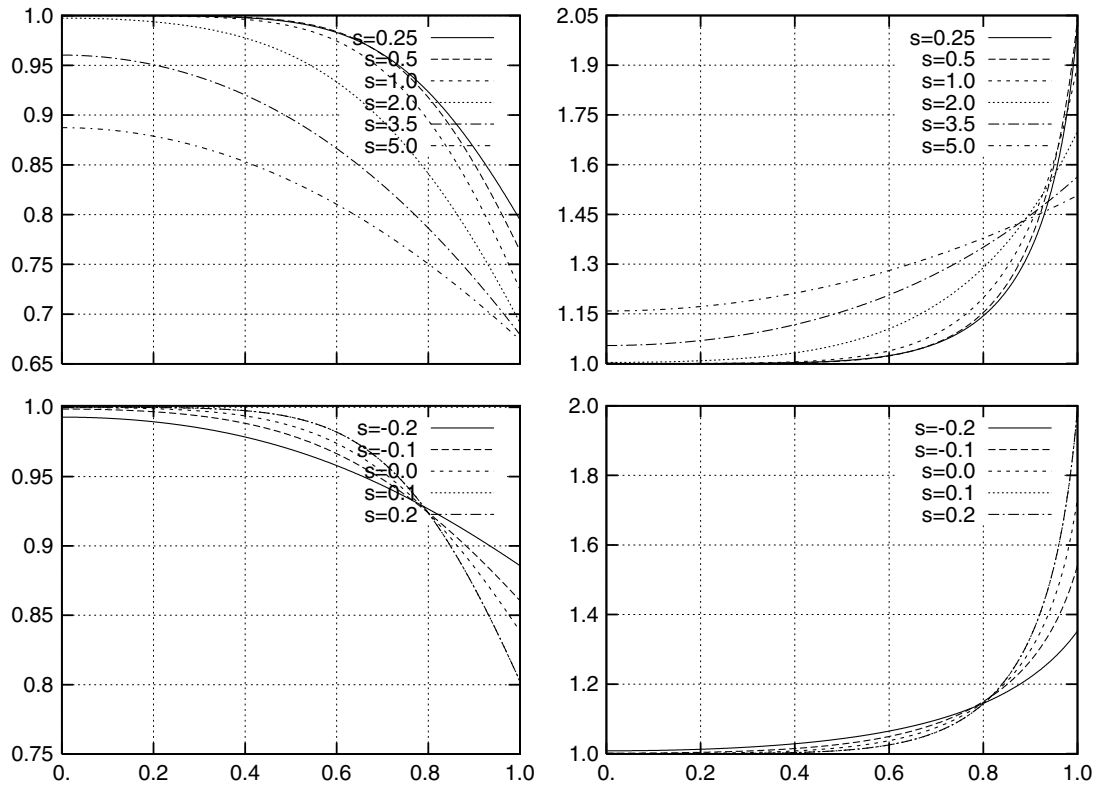


Fig. 4. The profiles of v for $p = 4$ and $t = 0.1$. Upper panels: $0.25 \leq s \leq 5$ Lower panels: $-0.2 \leq s \leq 0.2$. Left panels: emissivity b.c. Right panels: energy input at the boundary.

It is also important to investigate the role of the parameters s and p on the behavior of the solution. We mention (see, e.g. [2,4,5]) that, the most often encountered case in physics is that the heat-conduction coefficient K depends on the fourth power of the temperature i.e. $p = 4$. For this reason, we chose $p = 4$ and ran calculations for different s . It is known that the heat capacitance C is not as strong function of temperature as the heat conduction, K . This means the s is close to zero, i.e. the range $-0.2 < s < 5$ is fully adequate. Then the range for the power in the time dependent term α , is $3.5 > \alpha > -0.167$.

One is to expect that for larger α the evolution will be more nonlinear. Indeed, the upper panels of Fig. 3 demonstrate this kind of dependence for a smaller time $t = 0.05$, the most deformed curves are for the smallest $s \approx 0.5$ ($\alpha \approx 2.333$). Once again, the energy feedback (for $\sigma = +1$) leads to blow up of the solution (right panels) and the blow-up is fastest at the boundary.

What we found to be counterintuitive is that for $s < 0.25$ ($\alpha > 3.167$) this trend is reversed, and the smaller s (larger α) have smoother curves. This means that for large enough α 's the behaviours once ageing resembles the evolution in a linear heat equation. This is seen in the lower panels of Fig. 3. The conclusion is that the most nonlinear behavior for $p = 4$ is observed around $s \approx 0.5$ ($\alpha \approx 2.333$).

For completeness, we show in Fig. 4 the same cases but for twice longer time, $t = 0.1$. The general tendency is the same, but the profiles become more prolate due to the action of dissipation.

7. Conclusion

In this paper we consider the heat-conduction equation with nonlinear capacitance and diffusion coefficients. One of the boundary conditions is strongly nonlinear involving the Stephan–Boltzmann emission law. We consider two different implementations of the latter: emissivity at the boundary and energy influx. We apply the so-called equivalence transformation to make the diffusion term for the new variable linear. This

is important both for the qualitative theoretical investigation and for the numerical implementation. The new formulation allowed us to show that a balance law holds for a specially formulated functional of the unknown function. We created a special difference scheme that faithfully represents the balance law that holds for the continuous systems. We investigated the dynamics of the process for different values of the governing parameters. The case with energy influx invariable led to blow-up at the boundary, while the emissivity condition ensured that the function decay to zero for sufficiently large times. We show that the nonlinear boundary condition acts to make the profile steeper near the boundary. We investigated the interplay between the nonlinearity of the heat capacitance and diffusivity. Results are presented graphically.

Acknowledgements

M.A.C. would like to express his gratitude to the Cyprus Research Promotion Foundation for support through the Grant CRPF/0504/02. C.I.C acknowledges an invitation from the University of Cyprus, and the hospitality of the group of Prof. C. Sophocleous. The authors also wish to thank the referees for their suggestions for the improvement of this paper.

References

- [1] M.L. Storm, Heat conduction in simple metals, *J. Appl. Phys.* 22 (1951) 940–951.
- [2] G. Rosen, Nonlinear heat conduction in solid H_2 , *Phys. Rev. B* 19 (1979) 2398–2399.
- [3] J. Crank, *The Mathematics of Diffusion*, Oxford University Press, Oxford, 1975.
- [4] T.W. Davies, Transient conduction in a sphere with counteracting radiative and convective heat transfer at the surface, *Appl. Math. Model.* 12 (1988) 429–433.
- [5] T.W. Davies, Transient conduction in a plate with counteracting convection and thermal radiation at the boundary, *Appl. Math. Model.* 9 (1985) 337–340.
- [6] M. Koizumi, M. Utamura, K. Kotani, Three-dimensional transient heat conduction analysis with non-linear boundary conditions by boundary element method, *J. Nucl. Sci. Technol.* 22 (1985) 972–982.
- [7] P.R. Wallace, *Mathematical Analysis of Physical Problems*, Dover, New York, 1984.
- [8] M.B. Abd-el-Malek, M.M. Helal, Group method solution for solving nonlinear heat diffusion problems, *Appl. Math. Model.* 30 (2006) 930–940.
- [9] L.V. Ovsiannikov, *Group Analysis of Differential Equations*, Academic Press, New York, 1982.
- [10] J.G. Kingston, C. Sophocleous, On form-preserving point transformations of partial differential equations, *J. Phys. A: Math. Gen.* 31 (1998) 1597–1619.
- [11] O.O. Vaneeva, J.G. Jonhpillai, R.O. Popovych, C. Sophocleous, Enhanced group analysis and conservation laws of variable coefficient reaction diffusion equations with power nonlinearities, *J. Math. Anal. Appl.* 330 (2007) 1363–1386.
- [12] R.O. Popovych, N.M. Ivanova, New results on group classification of nonlinear diffusion–convection equations, *J. Phys. A* 37 (2004) 7547–7565.
- [13] C.I. Christov, K. Deng, Numerical investigation of quenching for a nonlinear diffusion equation with singular Newman condition, *Int. J. Numer. Methods Partial Differen. Eq.* 18 (2002) 429–440.
- [14] A.A. Samarskii, *The Theory of Difference Schemes*, Marcel Dekker, New York, 2001.